Supplementary information

**Regulation of Grain Boundary CeFe$_2$ Phase via Cu Addition for Anisotropic Ce-Fe-B Magnet Fabrication**

Guang Yu[1,†], Shuainan Xu[1,†], Xuefeng Liao[3], Bang Zhou[1,2], Hongya Yu[1], Xichun Zhong[1], Zhongwu Liu[1,*]

[1] *School of Materials Science and Engineering, South China University of Technology, Guangzhou 510640, China*

[2] *Advanced Materials Institute, Shenzhen International Graduate School, Tsinghua University, Shenzhen 518055, China*

[3] *Guangdong Provincial Key Laboratory of Rare Earth Development and Application, Institute of Resources Utilization and Rare Earth Development, Guangdong Academy of Sciences, Guangzhou 510650, China*
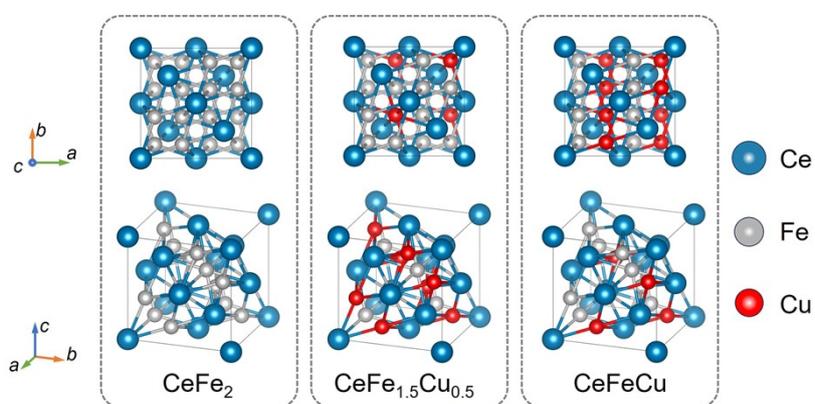
**Figure S1** Schematic illustration of the CeFe$_{2-x}$Cu$_x$ (x = 0, 0.5 and 1.0) crystal structure

† Guang Yu and Shuainan Xu contributed equally in this work.
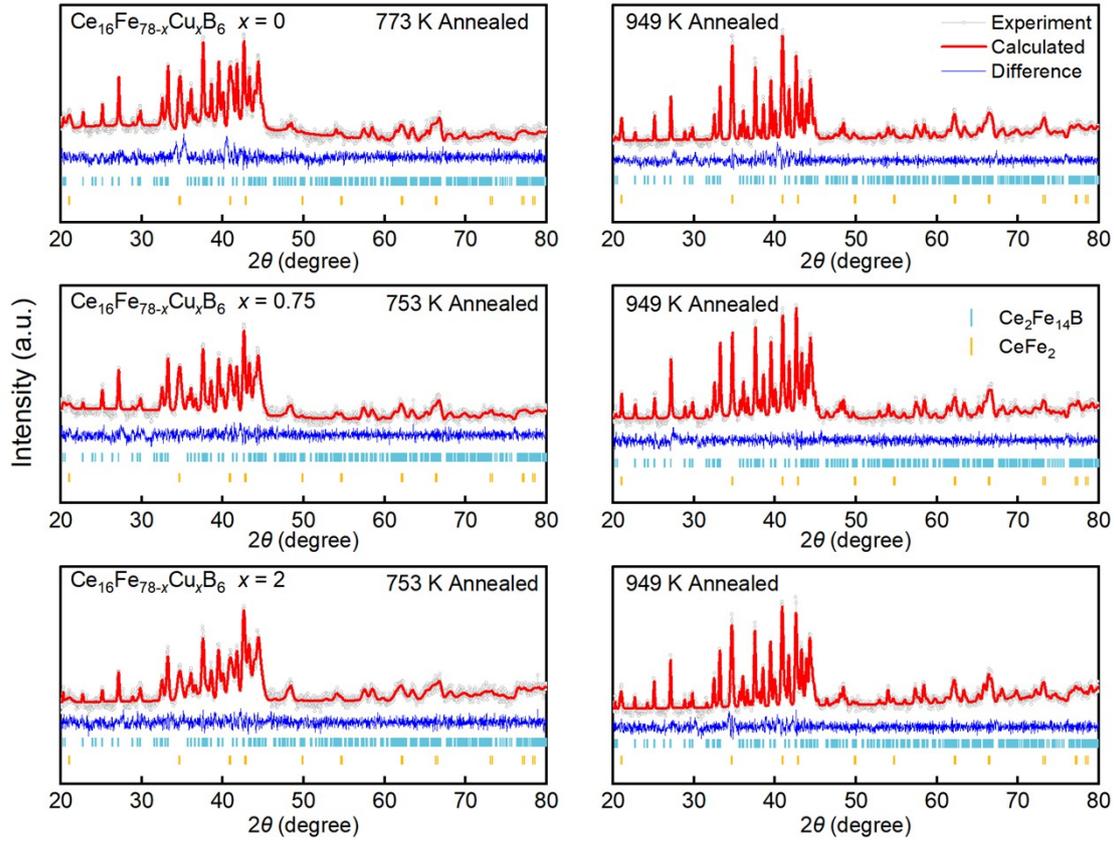
Figure S2 The Rietveld refinement of XRD patterns for the $Ce_{16}Fe_{78-x}Cu_xB_6$ amorphous alloys after annealing treatment ($x = 0$, 0.75 and 2.0 at.%)

Table S1 the refined lattice parameters of annealed $Ce_{16}Fe_{78-x}Cu_xB_6$ alloys in Figure S2

| x content (at.%)	Annealed Temp. (K)	$Ce_2Fe_{14}B$			$CeFe_2$	Mass Fraction(wt.%)		Rietveld Refinement Parameters		
		a (Å)	c/a	c (Å)	a (Å)	$Ce_2Fe_{14}B$	$CeFe_2$	R_p	R_{wp}	χ^2
0	773	8.76	1.38	12.12	7.32	94.56	5.44	3.03	4.54	1.75
	949	8.75	1.38	12.11	7.31	92.50	7.50	3.27	4.83	1.76
0.75	753	8.75	1.38	12.11	7.31	97.78	2.22	3.03	4.54	1.75
	949	8.75	1.38	12.11	7.3	92.25	7.75	3.66	5.26	2.28
2	753	8.75	1.38	12.11	7.3	97.28	2.72	4.09	5.12	2.32
	949	8.75	1.38	12.11	7.3	96.55	3.45	3.1	4.79	1.89
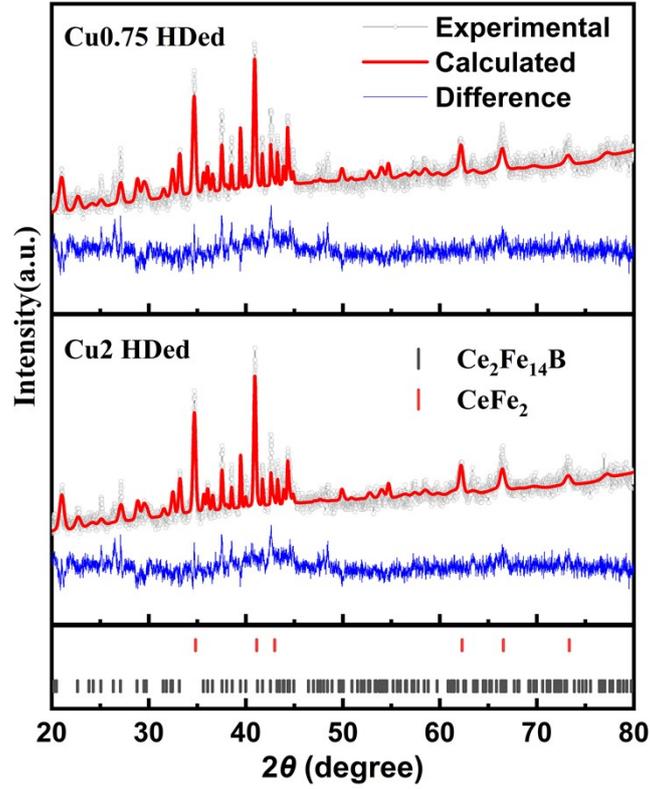
Figure S3 The Rietveld refinement of XRD patterns of the $Ce_{16}Fe_{78-x}Cu_xB_6$ hot-deformed magnets ($x = 0.75$ and 2.0 at.%).

Table S2 he refined lattice parameters of $Ce_{16}Fe_{78-x}Cu_xB_6$ hot-deformed magnets in Figure S3

| x content□(at.%)	$Ce_2Fe_{14}B$			$CeFe_2$	
	a (Å)	c/a	c (Å)	a (Å)	Cell Volume
.75	8.75	1.38	12.11	7.31	390.69
2	8.75	1.39	12.12	7.31	390.84
□x content□(at.%)	Mass Fraction(wt.%)		Rietveld Refinement Parameters		
	$Ce_2Fe_{14}B$	$CeFe_2$	R_p	R_{wp}	χ^2
0.75	94.56	5.44	4.26	5.54	2.48
2	92.5	7.5	4.03	5.23	2.32
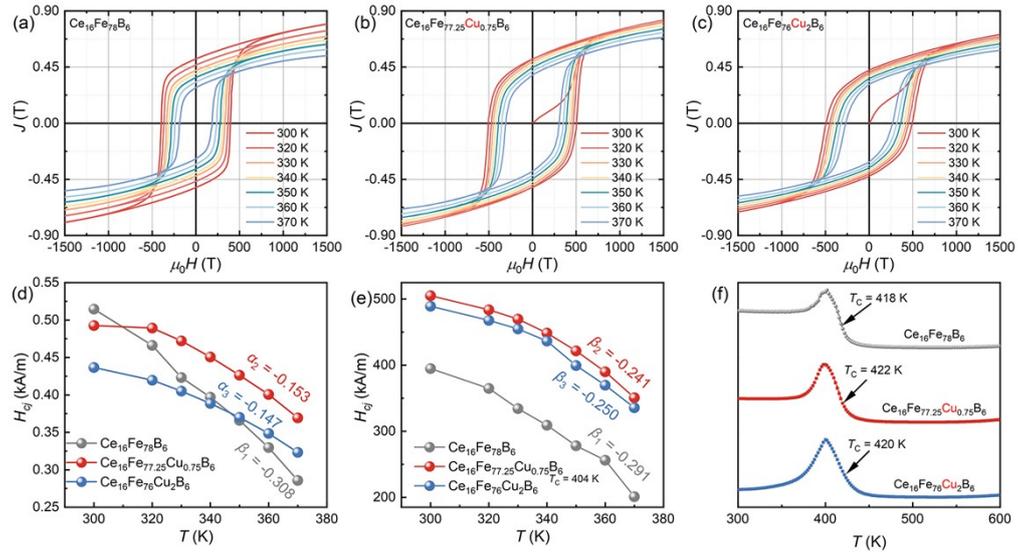
Figure S4 Curie temperature and high-temperature performance of Cu-doped $Ce_{16}Fe_{78-x}Cu_xB_6$ alloys (x = 0.75 and 2.0 at.%) and $Ce_{16}Fe_{76}Cu_2B_6$ hot-deformed magnets.
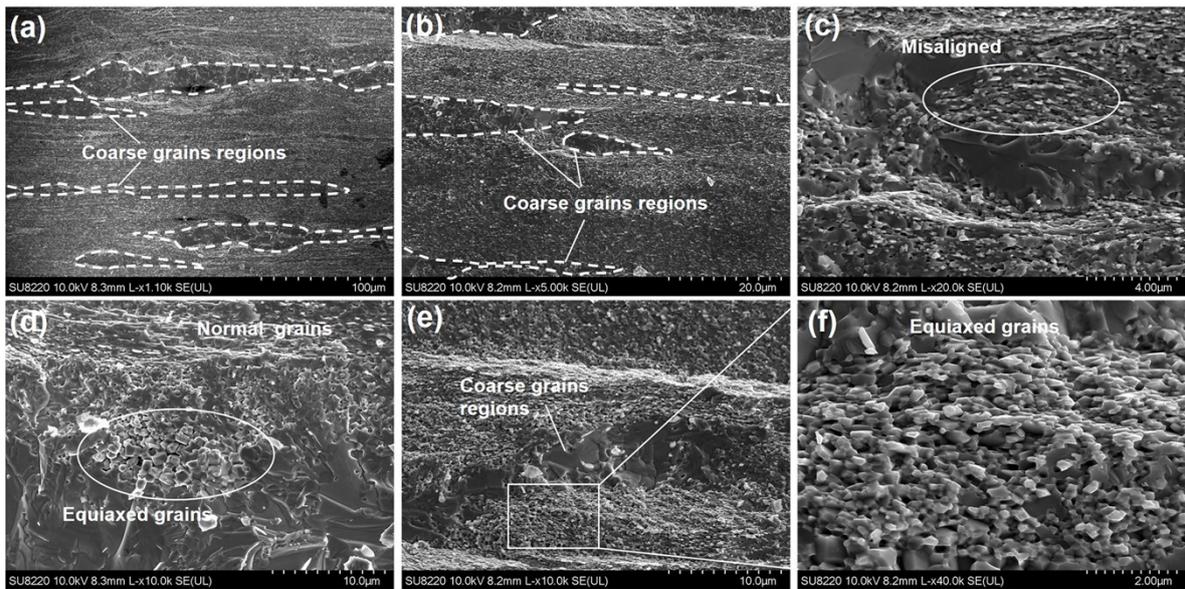
Figure S5 Microstructural characterization of the $Ce_{16}Fe_{76}Cu_2B_6$ hot-deformed magnets.
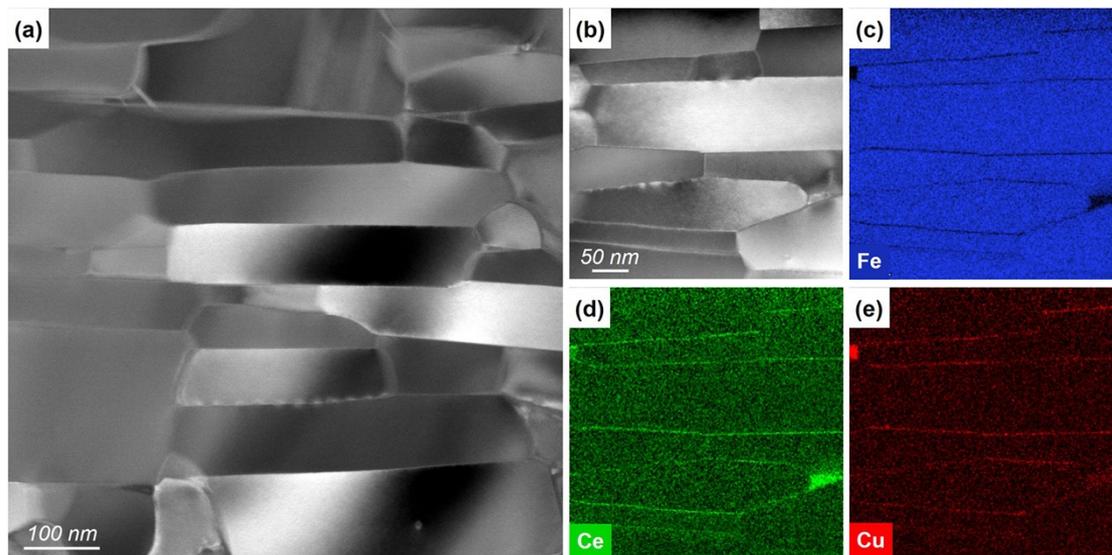
Figure S6 Microstructural characterization of the $Ce_{16}Fe_{76}Cu_2B_6$ hot-deformed magnets.